

# Conductive Inkjet-Printed Antennas on Flexible Low-Cost Paper-Based Substrates for RFID and WSN Applications

*Amin Rida, Li Yang, Rushi Vyas, and Manos M. Tentzeris*

Georgia Institute of Technology  
Atlanta, GA 30309 USA  
E-mail: arida@gatech.edu

---

## Abstract

In this paper, a review of the authors' work on inkjet-printed flexible antennas, fabricated on paper substrates, is given. This is presented as a system-level solution for ultra-low-cost mass production of UHF radio-frequency identification (RFID) tags and wireless sensor nodes (WSN), in an approach that could be easily extended to other microwave and wireless applications. First, we discuss the benefits of using paper as a substrate for high-frequency applications, reporting its very good electrical/dielectric performance up to at least 1 GHz. The RF characteristics of the paper-based substrate are studied by using a microstrip-ring resonator, in order to characterize the dielectric properties (dielectric constant and loss tangent). We then give details about the inkjet-printing technology, including the characterization of the conductive ink, which consists of nano-silver particles. We highlight the importance of this technology as a fast and simple fabrication technique, especially on flexible organic (e.g., LCP) or paper-based substrates. A compact inkjet-printed UHF "passive RFID" antenna, using the classic T-match approach and designed to match the IC's complex impedance, is presented as a demonstration prototype for this technology. In addition, we briefly touch upon the state-of-the-art area of fully-integrated wireless sensor modules on paper. We show the first-ever two-dimensional sensor integration with an RFID tag module on paper, as well as the possibility of a three-dimensional multilayer paper-based RF/microwave structure.

**Keywords:** RFID; ink jet printing; paper insulation; paper-based substrate; UHF antennas; microstrip antennas; printed antennas; low-cost RF modules; printable electronics; sensor integration; microsensors

## 1. Introduction

**R**FID is an emerging compact wireless technology for the identification of objects. It is considered an eminent candidate for the realization of completely ubiquitous "ad hoc" wireless networks. RFID utilizes electromagnetic waves for transmitting and receiving information stored in a tag or transponder to and from a reader. This technology has several benefits over the conventional methods of identification, such as a higher reading range, faster data transfer, the ability of RFID tags to be embedded within objects, no requirement for line of sight, and the ability to simultaneously read a massive amount of tags [1]. A listing of applications that currently use RFID includes the retail supply chain, the military supply chain, pharmaceutical tracking and management, access control, sensing and metering applications, parcel and document tracking, automatic payment solutions, asset tracking, real-time location systems (RTLS), automatic vehicle identification, and livestock or pet tracking.

The demand for flexible RFID tags has recently increased tremendously, due to the requirements for automatic identification, tracking, and monitoring in the various areas listed above. Compared with the lower-frequency tags (LF and HF bands), which

already suffer from limited reading ranges (1-2 ft), RFID tags in the UHF band see the widest use, due to their higher reading range (over 10 ft) and higher data transfer rate [2]. The major challenges that could potentially hinder the practical implementation of RFID are:

1. **Cost:** in order for RFID technology to realize a completely ubiquitous network, the cost of the RFID tags has to be extremely inexpensive, in order for the technology to be realized in mass-production amounts;
2. **Reliability,** which extends primarily to the efficiency of the RFID-tag antennas, readers, and the middleware deployed;
3. **The regulatory situation,** meaning that tags have to abide to a certain global regulatory set of requirements, such as the bandwidth allocations of the Gen2 Protocols defined by the EPC Global regulatory unit [3]; and
4. **Environmentally friendly materials,** in order to allow for the easy disposal of a massive number (in the billions) of RFID tags.

This review article makes use of the results that have been previously published and presented [5-11, 16, 28-36] by the authors. It hence demonstrates how inkjet printing of antennas and matching networks on low-cost paper-based materials can tackle all four challenges, enabling the easy implementation of ubiquitous RFID and wireless sensor node networks. It starts by discussing why paper should be used as a substrate for UHF/wireless inlays. This is followed by the dielectric characterization of paper, using a microstrip-ring-resonator method. The article then shows how we can use conductive inkjet-printing technology for the fast fabrication of RF/wireless circuits, and provides a design guideline for an inkjet-printed broadband antenna for UHF RFID tags that can be used globally. The article shows the capability of integrating sensors with RFID tags, and discusses how this added functionality could revolutionize data fusion and real-time environmental cognition.

## 2. Paper: The Ultimate Solution for a Lowest-Cost Environmentally Friendly RF Substrate

There are many aspects of paper that make it an excellent candidate for an extremely low-cost substrate for RFID and other RF applications. Paper, an organic-based substrate, is widely available. The high demand and the mass production of paper make it the cheapest material ever made. From a manufacturing point of view, paper is well suited for reel-to-reel processing, as shown in Figure 1. The mass fabrication of RFID inlays on paper thus becomes more feasible. Paper also has a low surface profile. With an appropriate coating, it is suitable for fast printing processes, such as direct-write methodologies, instead of the traditional metal-etching techniques. A fast process, such as inkjet printing, can be used efficiently to print electronics on or in paper substrates. This also enables components such as antennas, ICs, memory, batteries, and/or sensors to be easily embedded in or on paper modules. In addition, paper can be made hydrophobic, as shown in Figure 2, and/or fire retardant by adding certain textiles to it. This can easily resolve any moisture-absorbing issues from which fiber-based materials, such as paper, suffer [4]. Last but not least, paper is one of the most environmentally friendly materials. The proposed approach could potentially set the foundation for the first generation of truly “green” RF electronics and modules.

However, there is wide availability of different types of paper, which vary in density, coating, thickness, texture, and, implicitly, dielectric properties, including dielectric constant and dielectric loss tangent. Due to this, dielectric RF characterization of paper substrates becomes an essential step before any RF “on-paper” designs. The electrical characterization of paper has already been performed [5, 7] by the authors, and results have shown the feasibility of the use of paper at UHF and RF frequencies..

Another note to mention here is that the low cost of fabrication, and even assembly with printed-circuit-board-compatible processes, can realize paper boards similar to printed wiring boards. These can support passives, wiring, RFID, sensors, and other components in a three-dimensional multilayer platform [5-10].

### 2.1 Dielectric Characterization of the Paper Substrate

RF characterization of paper becomes a critical step for the qualification of the paper material for a wide range of frequency-

domain applications. The knowledge of the dielectric properties, such as the dielectric constant ( $\epsilon_r$ ) and the loss tangent ( $\tan \delta$ ) become necessary for the design of any high-frequency structure, such as an RFID antenna on the paper substrate and, more importantly, if it is to be embedded inside the substrate. Precise methods for high-frequency dielectric characterization include microstrip-ring resonators, parallel-plate resonators, and cavity resonators [13]. In our extensive literature review, such properties were not found to be available for paper for the frequency range (above 900 MHz) of the desired application.

In order to measure the dielectric constant ( $\epsilon_r$ ) and loss tangent ( $\tan \delta$ ) of paper up to 2 GHz, a microstrip-ring resonator structure was designed. A diagram of the configuration is shown in Figure 3. The through-reflect-lines (TRL) calibration method was

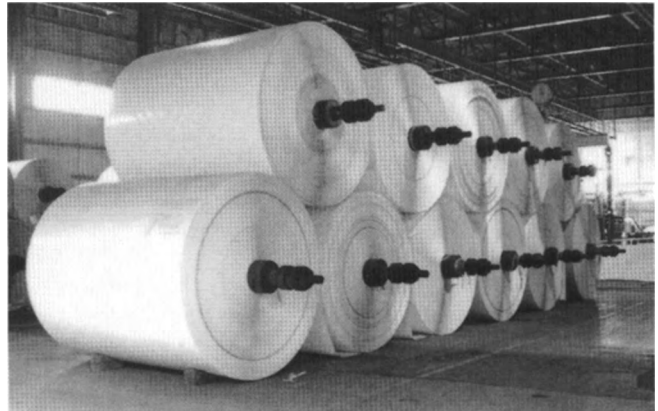


Figure 1. Reels of paper.

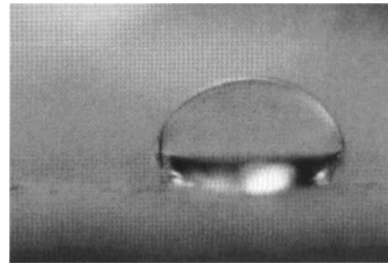


Figure 2. A magnified droplet of water sitting on a paper substrate.

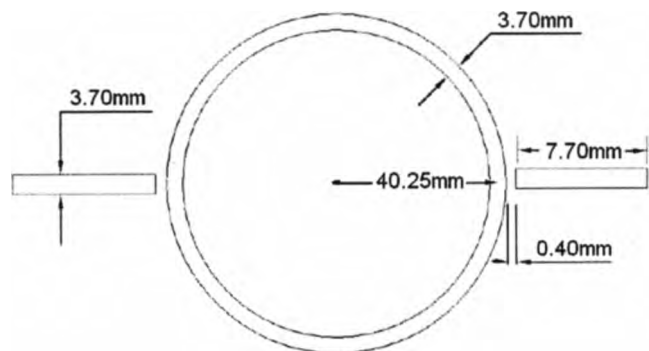


Fig. 3. A diagram of the configuration of the microstrip ring resonator.

utilized to de-embed the effect of the feeding lines. It is to be noted that extraction of  $\tan \delta$  using the microstrip-ring-resonator approach requires reliable theoretical equations for the estimation of the conductor losses [2, 12, 13].

Among the critical needs for the selection of the right type of paper for electronics applications are surface planarity, repelling of water, lamination capability for three-dimensional module development, the ability to form vias, adhesion, and the ability to co-process with low-cost manufacturing. For the trial runs, a commercially available paper with a hydrophobic coating was selected. The thickness of the single sheet of paper was  $260 \pm 3 \mu\text{m}$ . An 18  $\mu\text{m}$ -thick copper foil was selected as the metallic material. It was heat-bonded onto both sides of the paper substrate in order to accurately model and de-embed the conductive loss of the microstrip circuit. The photolithography process was conducted using a dry-film photo-resist, followed by UV exposure, and finally etching the copper using a slow-etching methodology. The paper substrate was then dried at  $100^\circ \text{C}$  for 30 min. To investigate the sensitivity of the results to the paper's thickness, as well as to investigate the effect of the bonding process, nine sheets of paper were directly heat-bonded together to produce a thickness of 2.3 mm, without any extra adhesive layers.

The characterization covered the UHF RFID frequency band, which is utilized by applications that are commonly used in port security, inventory tracking, airport security and baggage control, and the automotive, pharmaceutical, and healthcare industries.

The ring resonator produces insertion loss ( $S_{21}$ ) results with periodic frequency resonances. In this method,  $\epsilon$  can be extracted from the location of the resonances of a ring resonator of given radius. The value of  $\tan \delta$  is extracted from the quality factor ( $Q$ ) of the resonance peaks, along with the theoretical calculations of the conductor's losses. Measurements of  $S_{21}$  were done over the frequency range of 0.4 GHz to 1.9 GHz using an Agilent 8530A vector network analyzer (VNA). Typical SMA coaxial connectors were used to feed the ring-resonator structure. TRL calibration was performed to de-embed the effects of the input and output microstrip feeding lines, and to eliminate any impedance mismatch.

Figure 3 shows the layout of the ring resonator, along with the dimensions for the microstrip feeding lines, the gap in between the microstrip lines and the microstrip ring resonator, the width of the signal lines, and the mean radius,  $r_m$ . Figure 4 shows fabricated ring resonators with the TRL lines. Data for the magnitude of  $S_{21}$  as a function of frequency were then inserted into a *MATCAD* program, and the dielectric constant and loss tangent were extracted [5, 7, 11]. A plot of  $S_{21}$  as a function of frequency is shown in Figure 5.

## 2.1.1 Dielectric Constant

In order to extract the dielectric constant, the desired resonant peaks were first obtained according to [5, 11]

$$f_0 = \frac{nc}{2\pi r_m \sqrt{\epsilon_{eff}}}, \quad (1)$$

where  $f_0$  corresponds to the  $n$ th resonance frequency of the ring with a mean radius of  $r_m$  and an effective dielectric constant  $\epsilon_{eff}$ , with  $c$  being the speed of light in vacuum. The extracted values of  $\epsilon_r$  at 0.71 GHz and 1.44 GHz, shown in Figure 5, were obtained using Equation (1). They are shown in Table 1.

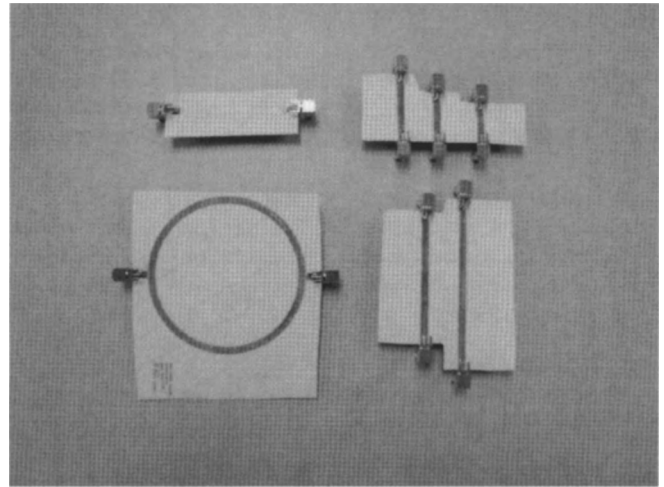


Fig. 4. A photo of fabricated microstrip ring resonators and TRL lines bonded to SMA connectors.

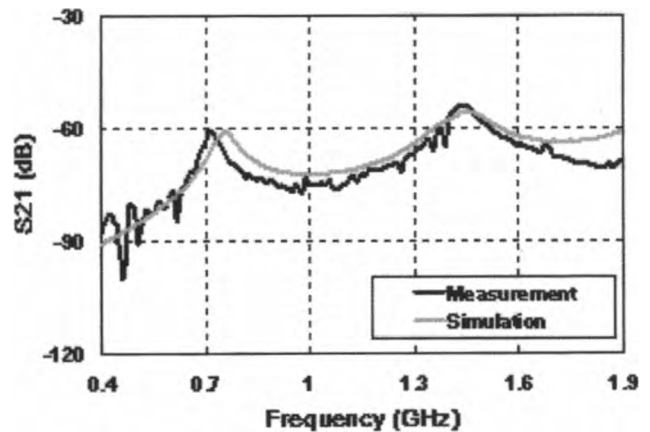


Figure 5.  $S_{21}$  as a function of frequency for the ring resonator.

Table 1. The extraction of the dielectric constant from the ring-resonator measurement.

Mode	Resonant Frequency $f_0$	Insertion Loss $ S_{21} $	$BW_{-3\text{dB}}$	$\epsilon_r$	$\tan \delta$
$n = 1$	0.71 GHz	-61.03 dB	42.12 MHz	3.28	0.061
$n = 2$	1.44 GHz	-53.92 dB	75.47 MHz	3.20	0.053

## 2.1.2 Dielectric Loss

The extraction of the loss tangent was performed by calculating the theoretical values of the conductor and radiation losses. This was done in order to isolate the dielectric loss,  $\alpha_d$ , since the ring-resonator method gives the total loss at the frequency locations of the resonant peaks. The loss tangent is a function of  $\alpha_d$  (in nepers/m), according to [13]

$$\tan \delta = \frac{\alpha_d \lambda_0 \sqrt{\epsilon_{eff}} (\epsilon_r - 1)}{\pi \epsilon_r (\epsilon_{eff} - 1)}, \quad (2)$$

where  $\lambda_0$  is the free-space wavelength, and  $\epsilon_r$  and  $\epsilon_{eff}$  are the same as described above. Available theoretical methods for calculating conductor loss and radiation loss have dated from the 1970s [13]. Results for  $\tan \delta$  are shown in Table 1, after subtracting the calculated conductor and radiation losses.

It is to be noted that the density of the paper substrate slightly increases after the bonding process described above [5, 9]. This may slightly increase the calculated dielectric properties in Table 1 for multilayer paper-based RF modules.

## 3. Conductive Inkjet Printing

Modern inkjet printers operate by propelling tiny droplets of liquid, of a size down to several pL [14, 18]. This new technology of inkjet printing [17, 19, 25], utilizing conductive paste, can rapidly fabricate prototype circuits, without iterations in photolithographic mask design or traditional etching techniques that have been widely used in industry. Printing is completely controlled from the designer's computer, and does not require a clean-room environment [13]. A droplet's volume determines the resolution of the printer. For example, a droplet of 10 pL gives a minimum thickness or gap size of printed traces and lines of  $\sim 25 \mu\text{m}$ . The cartridge consists of a piezo-driven jetting device, with integrated reservoir and heater [14, 18].

The inkjet printer used for this effort was a Dimatix Materials Printer DMP-2800, as shown in Figure 6. The inkjet printing was done as horizontal, bar-by-bar printing, using a DMC-11610 print head or cartridge, as shown in Figure 7. This print head has a nominal drop volume of 10 pL.

Unlike etching, which is a subtractive method of removing unwanted metal from the substrate's surface, inkjet printing jets the single ink droplet from the nozzle to the desired position. Therefore, no waste is created, resulting in an economical fabrication solution. Silver nano-particle inks are usually selected in the inkjet-printing process, to ensure good metal conductivity. After the silver nano-particle droplet is driven through the nozzle, a sintering process is found to be necessary, to remove excess solvent and to remove material impurities from the depositions. The sintering process also provides the secondary benefit of increasing the bond of the deposition to the paper substrate [15]. The conductivity of the conductive ink varies from 0.4 to  $2.5 \times 10^7 \text{ S/m}$ , depending on the temperature and duration of the curing. Figure 8 shows the difference between heating temperatures of  $100^\circ \text{C}$  and  $150^\circ \text{C}$  after 15 minutes of curing. At the lower temperature, larger gaps exist between the particles, resulting in a poor connection. When the

temperature is increased, the particles begin to expand, and gaps start to diminish. That guarantees a virtually continuous metal conductor, providing a good percolation channel in which the conduction electrons can flow. To ensure the conductivity performance of microwave circuits, such as RFID modules, curing temperatures around  $120^\circ \text{C}$  and curing durations of two hours were chosen in the following fabrication, to sufficiently cure the nano-particle ink. Alternatively, much shorter UV heating approaches can achieve similar results.

The savings in fabrication and prototyping time that inkjet printing brings to RF and wireless circuits is very critical to today's ever-changing electronics market. These savings verify inkjet printing's feasibility as an excellent prototyping and mass-production technology for next-generation electronics, especially in RFID, wireless sensors, handheld wireless devices (e.g., 4G and 4.5G cell phones), flexible circuits, and even in thin-film batteries [30, 32].

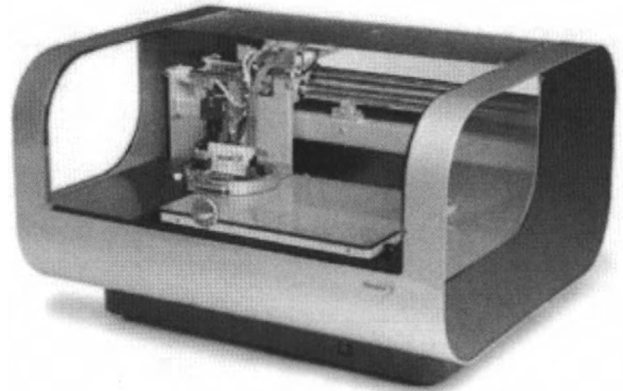


Figure 6. The DMP 2800 Dimatix Material Printer.

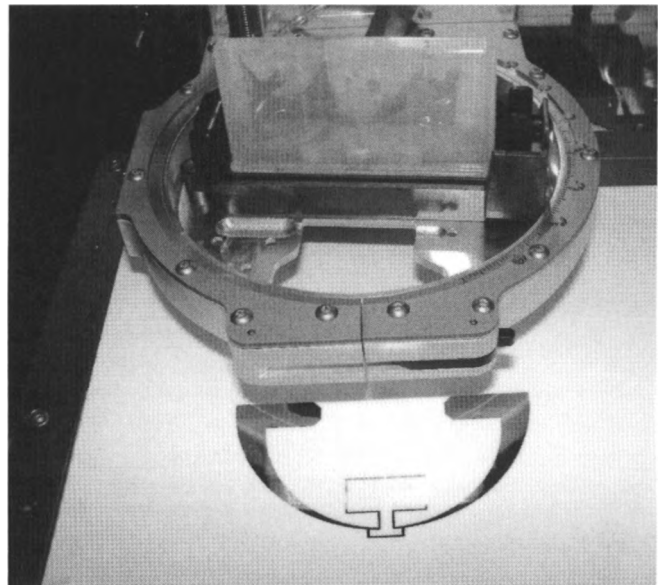


Figure 7. The DMC-11610 print head.

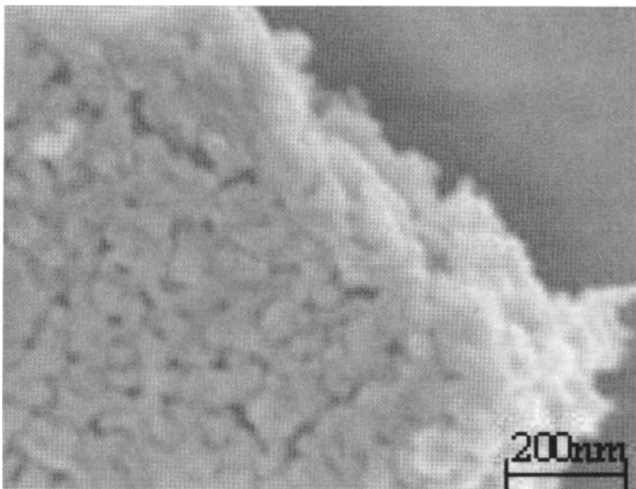
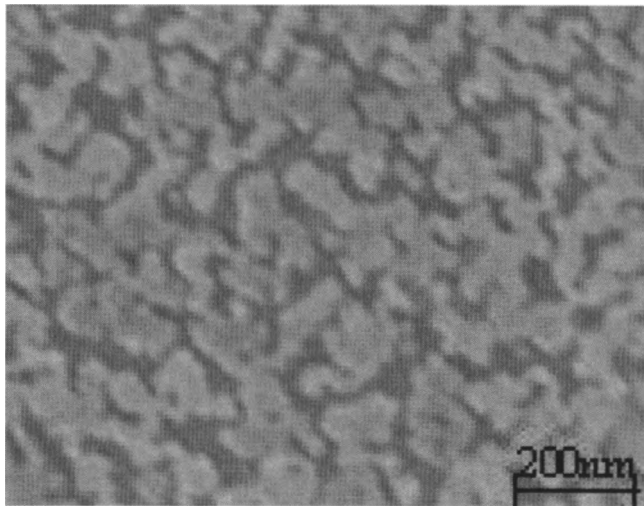


Figure 8. Scanning electron microscope images of a layer of printed silver nano-particle ink, after curing for 15 minutes at 100° C (top) and 150° C (bottom).

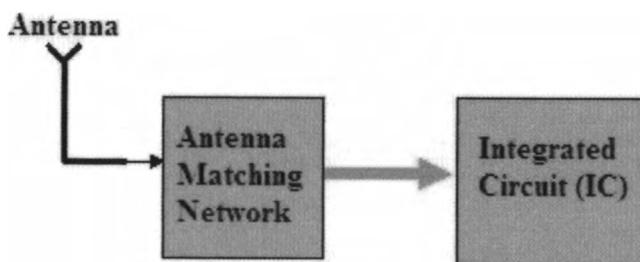


Figure 9. A block diagram of a passive RFID tag.

#### 4. A Benchmarking Prototype: A UHF RFID Antenna Design

A major challenge in RFID antenna design is the impedance matching of the antenna ( $Z_{ANT}$ ) to that of the IC ( $Z_{IC}$ ). For years, antennas have been designed primarily to match load of either  $50 \Omega$  or  $75 \Omega$ . However, RFID chips primarily exhibit complex input impedances, making matching extremely challenging [1].

It is to be noted that besides impedance matching, low cost, an omnidirectional radiation pattern, a long reading range, wide bandwidth, flexibility, and miniaturized size are all important features that an RFID tag must acquire. Most available commercial RFID tags are passive, due to cost and fabrication requirements. A purely passive RFID system utilizes the electromagnetic power transmitted by the reader antenna in order to power up the IC of the RFID tag, and to transmit back the tag's information to the reader using backscatter phenomena. A block diagram of a passive RFID tag is shown in Figure 9. The antenna-matching network must provide maximum power delivered to the IC, which is used to store the data that is transmitted to and received from the reader.

For truly global operation of passive UHF RFIDs, Gen2 protocols define different sets of frequencies, power levels, numbers of channels, and spurious sideband limits for the RFID reader's signal. These apply for different regions of operation: North America, 902-928 MHz; Europe, 866-868 MHz; Japan, 950-956 MHz; and China, 840.25-844.75 MHz and 920.85-924.75 MHz. This places a demand on the design of RFID tags to operate at all of those frequencies. This in turn requires a miniaturized broadband UHF antenna. For instance, in a scenario where cargo or containers are imported and exported from different regions of the world using a secure RFID-system implementation, an RFID tag is required to have a bandwidth wide enough to operate globally. This imposes very stringent design challenges for the antenna designers [26, 27].

To achieve these design goals – while demonstrating the exceptional capabilities of the paper-based inkjet-printed antenna technology – a T-match folded-bowtie half-wavelength dipole antenna [5, 20, 21] was designed and fabricated on a commercial photo paper using the inkjet printer mentioned above. The antenna used for this design was designed using Ansoft's *HFSS* three-dimensional EM solver. This design was used for matching the passive antenna terminals to a TI RI-UHF-Strap-08 IC, with a resistance of  $R_{IC} = 380 \Omega$ , and a reactance modeled by a capacitor with a value  $C_{IC} = 2.8 \text{ pF}$  [22]. The IC was modeled in *HFSS* by introducing a lumped port and an RLC boundary. The lumped port was specified to be a purely resistive source with  $R = 380 \Omega$ . The RLC boundary was specified to have a capacitance value of 2.8 pF, hence simulating the IC's complex impedance. The RFID prototype structure, along with dimensions, is shown in Figure 10, with the IC placed in the center of the T-match arms. The T-match arms are also responsible for matching the impedance of the antenna terminals to that of the IC, through the fine tuning of the length,  $L_3$ , the height,  $h$ , and the width,  $W_3$ . The current distribution on this antenna at 900 MHz is shown in Figure 11.

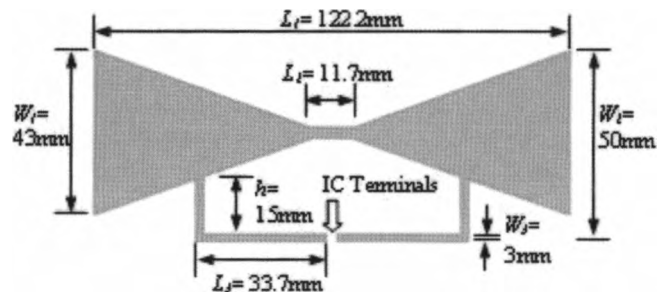


Figure 10. The configuration of the T-match folded-bowtie RFID tag module.

A GS 1000  $\mu\text{m}$ -pitch probe, connected to a UHF balun to ensure a balanced signal between the arms of the T-match folded-dipole antenna, was used for impedance measurements, as shown in Figure 12. In order to minimize backside reflections from this type of antenna, the fabricated inkjet printed antennas were placed on a custom-made probe station. This used high-density polystyrene foam, with a low dielectric-constant value of 1.06, resembling that of free space [23]. The calibration method used was short-open-load-through (SOLT). Figure 13 shows the impedance plots. As shown in Figure 13a, the simulated resistance for the antenna in the UHF RFID frequency range maintained a value close to 380  $\Omega$  between the two successive peaks. The reactance part of the impedance, shown in Figure 13b, featured a positive value with a linear variation with frequency. This pertained to an inductance that conjugately matched – or, equivalently, canceled – the effect of the 2.8 pF capacitance of the IC. Fairly good agreement was found between the simulation and measurement results. The distortion is possibly due to the effect of the metal probe fixture.

The return loss of this antenna was calculated based on the power-reflection coefficient. This took into account the reactive part of the IC's impedance [24]:

$$|S^2| = \left| \frac{Z_{IC} - Z_{ANT}^*}{Z_{IC} + Z_{ANT}^*} \right|^2, \quad (3)$$

where  $Z_{IC}$  represents the impedance of the IC,  $Z_{ANT}$  is the impedance of the antenna terminals, and  $Z_{ANT}^*$  is its conjugate. The return-loss plot is shown in Figure 14. It demonstrated good agreement for both paper-metallization approaches. The nature of the bowtie shape of the half-wavelength dipole antenna body allowed for broadband operation. It had a designed bandwidth of 190 MHz, corresponding to 22% around the center frequency of 854 MHz, which covers the universal UHF RFID bands. It has to be noted that the impedance value of the IC stated above was provided only for the UHF RFID frequency, which extends from 850 MHz to 960 MHz. The return loss outside this frequency region, shown in Figure 14, may thus vary significantly, due to potential IC impedance variations with frequency.

In order to verify the performance of the ink-jet-printed RFID antenna, measurements were performed on a copper-metallized antenna prototype. This had the same dimensions and was fabri-

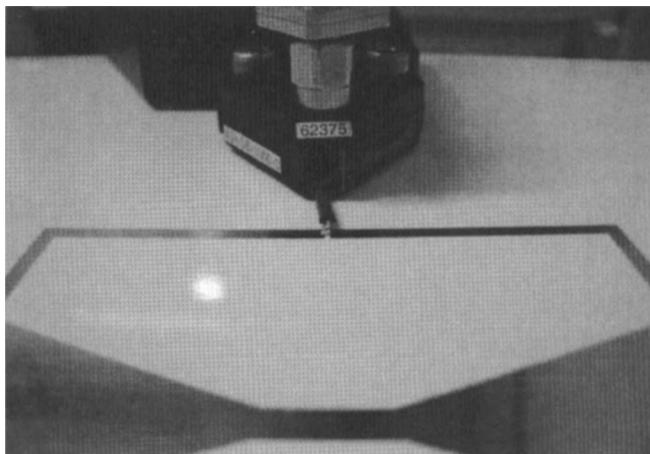


Figure 12. A photograph of the impedance measurement using the GS pitch probe.

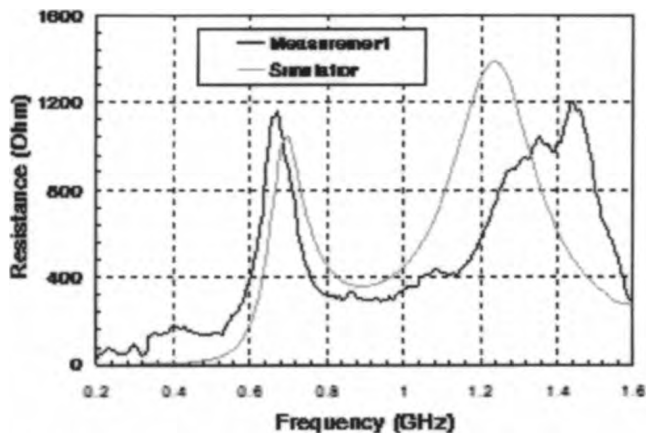


Figure 13a. The measured and simulated input resistance of the inkjet-printed RFID tag.

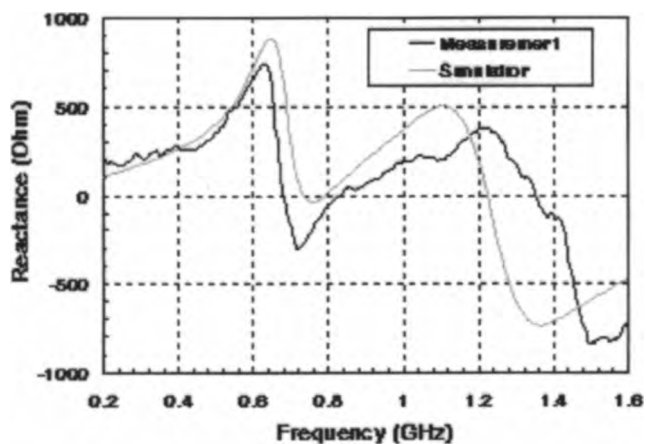


Figure 13b. The measured and simulated input reactance of the inkjet-printed RFID tag.

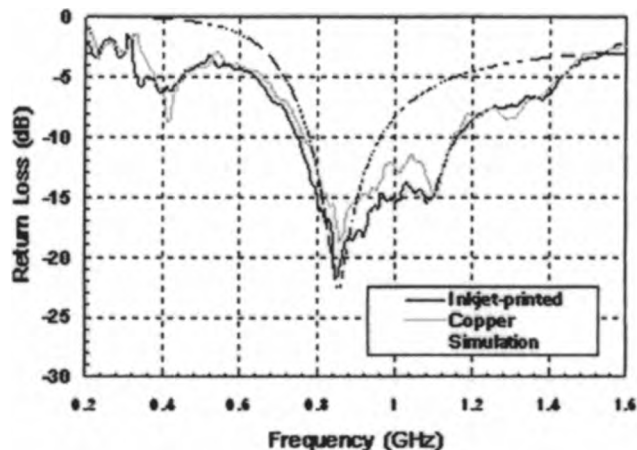
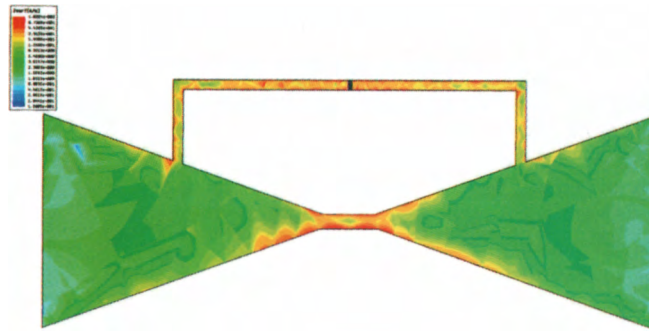
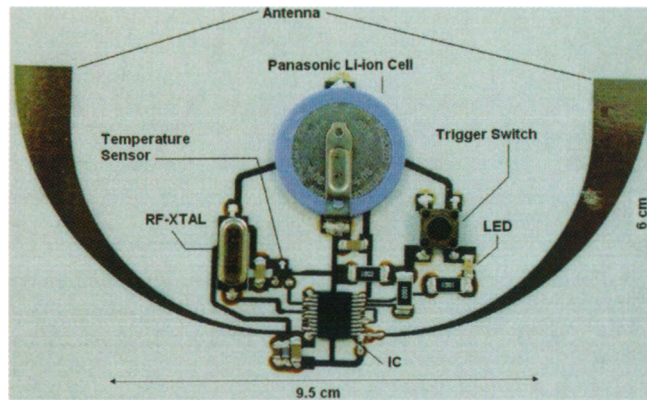


Figure 14. The measured and simulated return loss of the inkjet-printed RFID tag.



**Figure 11.** A simulation plot of the current distribution at 900 MHz.



**Figure 18.** The wireless-sensor transmitter prototype on a paper substrate, using silver inkjet-printing technology.

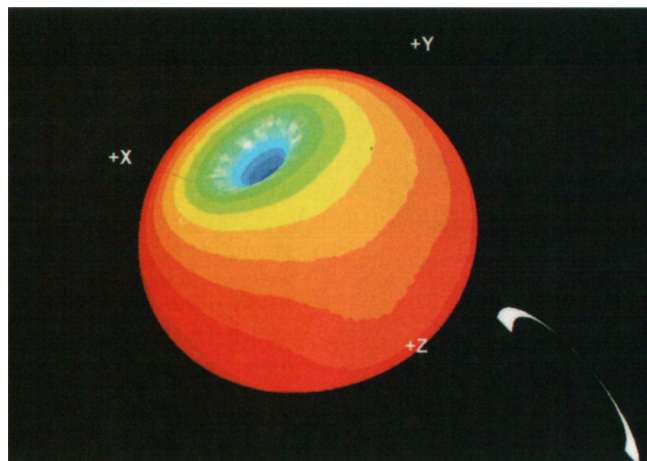


**Figure 19.** The measured normalized radiation pattern of the U-shaped antenna.

cated on the same paper substrate, using the slow-etching technique mentioned before. The return-loss results are included in Figure 14. They showed that the return loss of the inkjet-printed antenna was very slightly larger than the return loss of the copper antenna. Overall, good agreement between the copper-etched and the inkjet-printed antennas was observed, despite the higher metal loss of the silver-based conductive ink.

The radiation pattern was measured using Satimo’s Star-gate 64 antenna chamber measurement system, as shown in Figure 15. The NIST-calibrated SH8000 horn antenna was used as a calibration kit for the measured radiation pattern at 915 MHz. As shown in Figure 16, the radiation pattern was almost uniform (omnidirectional) at 915 MHz, with a directivity around 2.1 dBi. The IC strap was attached to the IC terminal with H2OE Epo-Tek silver conductive epoxy, cured at 80° C. A UHF RFID reader was used to detect the reading distance at different directions to the tag. These measured distances are theoretically proportional to the actual radiation pattern. The normalized radiation patterns of the simulation, the microwave-chamber measurement, and the reader measurement are plotted in Figure 16. They showed very good agreement between simulation and measurements, which also could be verified for other frequencies within the antenna’s bandwidth.

### 5. RFID/Sensor Integration

In addition to the basic RFID automatic identification capabilities and along with the technologies and designs discussed above, the authors have demonstrated the capabilities of inkjet-printing technology in integrated wireless sensors on paper, bridging RFID and sensing technology [28-36]. The aim is to create a system that is capable not only of tracking, but also of monitoring. With this, real-time cognition of the status of a certain object will be made possible by the simple function of a sensor integrated into the RFID tag. The ultimate goal is to create a secured “intelligent network of RFID-enabled sensors.” For this effort, the authors have developed the first sensor-enabled RFID on paper that uses Gen2 protocols as the means of communication.

A microcontroller-enabled wireless sensor module was realized on a paper-based substrate. The system-level design for this

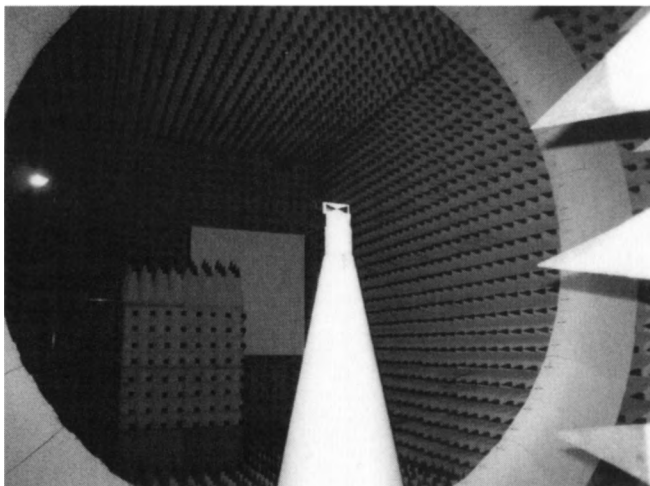


Figure 15. A photograph of the radiation-pattern measurement in an antenna chamber.

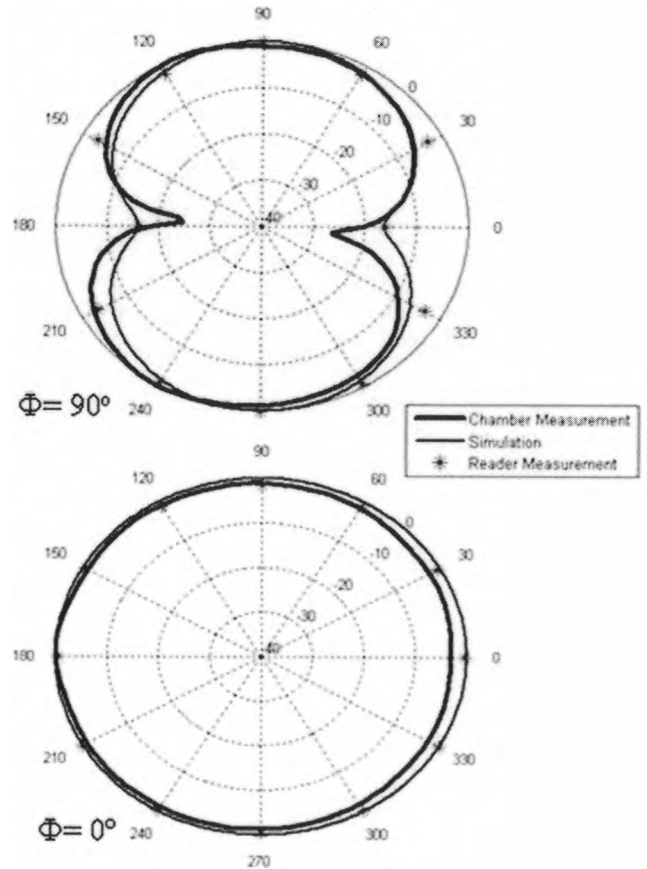


Figure 16. The normalized two-dimensional far-field radiation plots of the simulation results, the chamber measurements, and tag reading distance measurements.

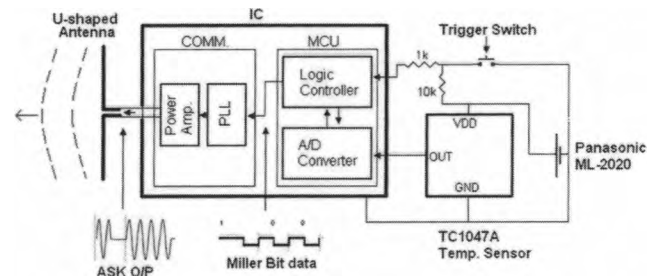


Figure 17. A system-level diagram of the wireless sensor module.

wireless transmitter can be seen in Figure 17. At the heart of the unit was an eight-bit integrated microcontroller unit that was programmed to sample an analog temperature sensor, to perform an analog-to-digital conversion of the sensed data, and to bit-encode the digital form of the sensed data into full two-subcarrier cycle Miller bits [3]. Finally, the power amplifier in the integrated transmitter module was modulated in the same sequence as the bit-encoded digital sensor data, using amplitude-shift keying (ASK) modulation. The transmission frequency of 904.4 MHz was generated by using a crystal oscillator, tied to the input of the phase-locked loop (PLL) unit of the transmitter. The data transmission was carried out on the unlicensed UHF frequency around 900 MHz.



The overall dimensions of the structure were 9.5 cm × 5 cm, and it is shown in Figure 18. Also shown are the antenna and the traces used for the assembled components: the TC1047 temperature sensor, the TSSOP packaged IC, inductors, capacitors, resistors, the crystal oscillator, and the battery. The return loss or  $S_{11}$  for the center frequency at the antenna's terminals was recorded to be -15.05 dB for the simulated structure using the HFSS full-wave EM simulator, and -12.45 dB measured using the ZVA-8 vector network analyzer. The normalized radiation pattern, shown in Figure 19, was also measured using Satimo's Stargate 64 antenna chamber measurement system, and using the NIST-calibrated SH8000 horn antenna as a calibration kit for the measured radiation pattern at 904 MHz. This prototype was tested for wireless transmission using an XR-400 RFID reader antenna, interfaced to a Tektronix RSA 3408A real-time spectrum analyzer (RTSA). The measured power was recorded to be -68 dBm.

This module could easily be extended to a three-dimensional multilayer paper-on-paper RFID/sensor module by laminating a number of photo-paper sheets (260 μm thickness per sheet). This is expected to drop the cost of the sensor nodes significantly, and to eventually made the "ubiquitous computing network" a possible reality, with a convergent ability to communicate, sense, and even process information.

## 6. Conclusion

Paper, which holds one of the biggest market shares in the world, can potentially revolutionize the electronics market. It could eventually take the first step in creating an environmentally friendly first generation of truly "green" RF electronics and modules. In addition, paper is one of the lowest-cost materials produced. Inkjet-printing technology – which is a much faster and cleaner method than conventional wet-etching techniques that use several "etchant" chemicals – can serve as a low-cost mass-deployment technology for fabricating RFID tags, produced in large reel-to-reel processes on paper. It can be easily verified that direct-write technologies, such as inkjet printing that consists of depositing nano-silver particles, can be a very critical technology for the quick development of next-generation flexible "cognitive" electronics, due to their speed and the ease of the prototyping process. A "global" UHF passive RFID antenna, using the classic T-match approach, has been presented as a benchmarking prototype for this novel technology. It featured excellent performance for a wide ("universal") frequency range. Last but not least, the authors have reported the first two-dimensional integrated sensor with UHF RFID capabilities completely on paper. This could potentially lay the foundation for truly convergent wireless-sensor ad hoc networks of the future.

## 7. References

1. K. Finkenzeller, *RFID Handbook, Second Edition*, New York, Wiley, 2004.
2. S. Basat, S. Bhattacharya, A. Rida, S. Johnston, L. Yang, M.M. Tentzeris, and J. Laskar, "Fabrication and Assembly of a Novel High-Efficiency UHF RFID Tag on Flexible LCP Substrate," Proceedings of the 56th IEEE-ECTC Symposium, May 2006, pp.1352-1355.
3. "UHF Gen-2 System Overview," Texas Instruments, September 2005, available at HTTP: [http://rfidusa.com/superstore/pdf/UHF\\_System\\_Overview.pdf](http://rfidusa.com/superstore/pdf/UHF_System_Overview.pdf).
4. M. Lessard, L. Nifterik, M. Masse, J. Penneau, and R. Grob, "Thermal Aging Study of Insulating Papers Used in Power Transformers," IEEE Electrical Insulation and Dielectric Phenomena 1996, 2, 1996, pp. 854-859.
5. L. Yang, A. Rida, R. Vyas, and M. M. Tentzeris, "RFID Tag and RF Structures on a Paper Substrate Using Inkjet-Printing Technology," IEEE Transactions on Microwave Theory and Techniques, 55, 12, December 2007, pp. 2894-2901.
6. A. Rida, L. Yang, R. Vyas, S. Basat, S. Bhattacharya, and M. M. Tentzeris "Novel Manufacturing Processes for Ultra-Low-Cost Paper-Based RFID Tags With Enhanced 'Wireless Intelligence'," Proceedings of the 57th IEEE-ECTC Symposium, Sparks, NV, June 2007, pp. 773-776.
7. L. Yang and M. M. Tentzeris, "3D Multilayer Integration and Packaging on Organic/Paper Low-Cost Substrates for RF and Wireless Applications," ISSSE '07 International Symposium on Signals, Systems and Electronics, July 30-August 2, 2007, pp. 267-270.
8. M. M. Tentzeris, L. Yang, A. Rida, A. Traille, R. Vyas, and T. Wu, "RFID's on Paper using Inkjet-Printing Technology: Is it the First Step for UHF Ubiquitous 'Cognitive Intelligence' and 'Global Tracking'?", RFID Eurasia, September 5-6, 2007, pp. 1-4.
9. A. Rida, R. Vyas, S. Basat, A. Ferrer-Vidal, L. Yang, S. Bhattacharya, and M. M. Tentzeris, "Paper-Based Ultra-Low-Cost Integrated RFID Tags for Sensing and Tracking Applications" Electronic Components and Technology Conference, May 29-June 1, 2007, pp. 1977-1980.
10. M. M. Tentzeris, L. Yang, A. Rida, A. Traille, R. Vyas, and T. Wu, "Inkjet-Printed RFID Tags on Paper-based Substrates for UHF "Cognitive Intelligence" Applications," IEEE International Symposium on Personal, Indoor and Mobile Radio Communications, September 3-7, 2007, pp. 1-4.
11. A. Rida, L. Yang, R. Vyas, S. Bhattacharya, and M. M. Tentzeris, "Design and Integration of Inkjet-Printed Paper-Based UHF Components for RFID and Ubiquitous Sensing Applications," IEEE European Microwave Conference, October 2007, pp. 724-727.
12. G. Zou, H. Gronqvist, J. P. Starski, and J. Liu, "Characterization of Liquid Crystal Polymer for High Frequency System-on-a-Package Applications," IEEE Transactions on Advanced Packaging, 25, 4, November 2002, pp. 503-508.
13. D. Thompson, O. Tantot, H. Jallageas, G. Ponchak, M. M. Tentzeris, and J. Papapolymerou, "Characterization of LCP Material and Transmission Lines on LCP Substrates from 30 to 110 GHz," IEEE Transactions on Microwave Theory and Techniques, 52, 4, April 2004, pp. 1343-1352.
14. Dimatix data sheet at <http://www.dimatix.com/files/DMP-2831-Datasheet.pdf>.
15. A. Pique and D. B. Chrisey, "Direct-Write Technologies for Rapid Prototyping Applications," New York, Academic Press, 2002, ISBN: 0-12-174231-8.

16. A. Traille, L. Yang, A. Rida, T. Wu, and M. M. Tentzeris, "Design and Modeling of Novel Multiband/Wideband Antennas for RFID Tags and Readers Using Time-/Frequency-Domain Simulators," Workshop on Computational Electromagnetics in Time-Domain, October 15-17, 2007, pp. 1-3.
17. M. Carter, J. Colvin, and J. Sears, "Characterization of Conductive Inks Deposited with Maskless Mesoscale Material Deposition," TMS2006, San Antonio, Texas, USA, March 12-16, 2006.
18. Fujifilm Dimatix Inc., "Piezo-electric inkjet print heads," <http://www.dimatix.com/markets/electronics.asp>.
19. O. Azucena, J. Kubby, D. Scarbrough, and C. Goldsmith, "Inkjet Printing of Passive Microwave Circuitry," IEEE MTT-S International Microwave Symposium Digest, June 15-20, 2008, pp. 1075-1078.
20. C. Balanis, *Antenna Theory, Analysis and Design, Third Edition*, New York, John Wiley & Sons, Inc., 2005.
21. R. A. Burberry, *VHF and UHF Antennas*, London, Peter Peregrinus Ltd., 1993.
22. Texas Instruments, "UHF Gen2 Strap RI-UHF-STRAP-08," data sheet, October 2006.
23. S. D. Kulkarni, R. M. Boisse, and S. N. Makarov, "A Linearly-Polarized Compact UHF PIFA with Foam Support," Department of Electrical Engineering, Worcester Polytechnic Institute, 2006.
24. P. V. Nikitin, S. Rao, S. F. Lam, V. Pillai, and H. Heinrich, "Power Reflection Coefficient Analysis for Complex Impedances in RFID Tag Design," *IEEE Transactions on Microwave Theory and Techniques*, **53**, 9, September 2005, pp. 2721-2725.
25. J. Siden, M. K. Fein, A. Koptyug, and H-E. Nilson, "Printed Antennas with Variable Conductive Ink Layers," *IET Proceedings on Microwaves, Antennas and Propagation*, **1**, 2, April 2007, pp. 401-407.
26. Y. Kurokawa, T. Ikeda, M. Endo, H. Dembo, D. Kawae, T. Inoue, M. Kozuma, D. Ohgarane, S. Saito, K. Dairiki, H. Takahashi, Y. Shionoiri, T. Atsumi, T. Osada, K. Takahashi, T. Matsuzaki, H. Takashina, Y. Yamashita, and S. Yamazaki, "UHF RF CPUs on Flexible and Glass Substrates for Secure RFID Systems," *IEEE Journal of Solid-State Circuits*, **43**, 1, January 2008, pp. 292-299.
27. Y. Kurokawa, T. Ikeda, M. Endo, H. Dembo, D. Kawae, T. Inoue, M. Kozuma, D. Ohgarane, S. Saito, K. Dairiki, H. Takahashi, Y. Shionoiri, T. Atsumi, T. Osada, K. Takahashi, T. Matsuzaki, H. Takashina, Y. Yamashita, and S. Yamazaki, "UHF RF CPUs on Flexible and Glass Substrates for Secure RFID Systems," 2007 IEEE International Solid-State Circuits Conference, ISSCC 2007, February 11-15, 2007, pp. 574-575.
28. L. Yang, S. Basat, A. Rida, and M. M. Tentzeris, "Design and Development of Novel Miniaturized UHF Tags on Ultra-low-cost Paper-Based Substrates," IEEE Asia Pacific Microwave Conference, December 2006, pp. 1493-1496.
29. A. Rida, L. Yang, and M. M. Tentzeris, "Design and Characterization of Novel Paper-Based Inkjet-Printed UHF Antennas for RFID and Sensing Applications," 2007 IEEE International Symposium on Antennas and Propagation, Honolulu, HI, July 2007, pp. 2749-2752.
30. S. Bhattacharya, M. M. Tentzeris, L. Yang, S. Basat, and A. Rida, "Flexible LCP and Paper-Based Substrates with Embedded Actives, Passives, and RFIDs," 2007 International Conference on Polymers and Adhesives in Microelectronics and Photonics, January 16, 2007, pp. 159-166.
31. L. Yang, A. Rida, T. Wu, S. Basat, and M. M. Tentzeris, "Integration of Sensors and Inkjet-Printed RFID Tags on Paper-Based Substrates for UHF 'Cognitive Intelligence' Applications," IEEE International Symposium on Antennas and Propagation, June 9-15, 2007, pp. 1193-1196.
32. A. Ferrer-Vidal, A. Rida, S. Basat, L. Yang, and M. M. Tentzeris, "Integration of Sensors and RFIDs on Ultra-Low-Cost Paper-Based Substrates for Wireless Sensor Networks Applications," IEEE Workshop on Wireless Mesh Networks, 2006 pp. 126-128.
33. A. Rida, R. Vyas, T. Wu, R. L. Li, and M. M. Tentzeris, "Development and Implementation of Novel UHF Paper-Based RFID Designs for Anti-Counterfeiting and Security Applications," IEEE International Workshop on Anti-Counterfeiting, Security, Identification, April 16-18, 2007, pp. 52-56.
34. L. Yang, A. Rida, J. Li, and M. M. Tentzeris, "Antenna Advancement Techniques and Integration of RFID Electronics on Organic Substrates for UHF RFID Applications in Automotive Sensing and Vehicle Security," IEEE Vehicular Technology Conference, September 30-October 3, 2007, pp. 2040-2041.
35. R. Vyas, A. Rida, L. Yang, and M. M. Tentzeris, "Design, Integration and Characterization of a Novel Paper Based Wireless Sensor Module," IEEE International Microwave Symposium, June 15-20, 2008, pp. 1305-1308.
36. R. Vyas, A. Rida, L. Yang, and M. M. Tentzeris, "Design and Development of First Entirely Paper Based Wireless Sensor Module," IEEE International Symposium on Antennas and Propagation, July 5-11, 2008, pp. 1-4.

## Introducing the Feature Article Authors



**Amin Rida** received his BS degree in Electrical Engineering from the Georgia Institute of Technology in May 2006, and is currently working toward the PhD degree. He is currently working at the Georgia Electronic Design Center. His research interests include characterization of organic substrates for RF applications, design of UHF antennas for RFID applications, and development of wireless transceivers for sensing and power scavenging applications. He was the recipient of the 2006 MTT-S Undergraduate/Pre-

Graduate Scholarship, recipient of the 2007 IEEE AP-S Symposium Best Student Paper Award, co-recipient of the 2007 ISAP Poster Presentation Award, and recipient of the 2006 Asian-Pacific Microwave Conference Award



**Li Yang** received the BS and MS degrees in Electronic Engineering from Tsinghua University, Beijing, China, in 2002 and 2005, respectively. He is currently pursuing his PhD in Electrical and Computer Engineering at the Georgia Institute of Technology, Atlanta. He is a Graduate Research Assistant with the ATHENA research group at the Georgia Electronic Design Center. His research interests include radio-frequency identification (RFID) technology, characterization of organic substrates for RF applications, and the design of wireless transceivers for sensing and power-scavenging applications. He was the recipient/co-recipient of the 2007 IEEE AP-S Symposium Best Student Paper Award, the 2007 IEEE IMS Third Best Student Paper Award, the 2007 ISAP Poster Presentation Award, and the 2006 Asian-Pacific Microwave Conference Award.



**Rushi Vyas** received his BS degree in Electrical and Computer Engineering from the Georgia Institute of Technology, Atlanta, in 2005, with a background in analog RF, power, and digital controllers. He is currently pursuing his PhD in Electrical and Computer Engineering at the Georgia Institute of Technology, Atlanta. He is a Graduate Research Assistant with the ATHENA research group at the Georgia Electronic Design Center in Atlanta. His research involves characterization of organic substrates for RF applications, and the design and development of wireless transceivers for sensing applications on organic substrates.



**Manos M. Tentzeris** received the Diploma Degree in Electrical and Computer Engineering from the National Technical University of Athens (Magna Cum Laude) in Greece, and the MS and PhD degrees in Electrical Engineering and Computer Science from the University of Michigan, Ann Arbor, MI. He is currently an Associate Professor with the School of ECE, Georgia Tech, Atlanta, GA.

Dr. Tentzeris has published more than 280 papers in refereed Journals and conference proceedings, two books, and 10 book chapters. He has helped develop academic programs in highly integrated/multilayer packaging for RF and wireless applications using ceramic and organic flexible materials, paper-based RFIDs and sensors, microwave MEMs, SOP-integrated (UWB, multi-band, conformal) antennas, and adaptive numerical electromagnetics (FDTD, multi-resolution algorithms) and heads the ATHENA research group (20 researchers). He is the Georgia Electronic Design Center Associate Director for RFID/sensors research. He was the Georgia Tech NSF-Packaging Research Center Associate Director for RF research and the RF Alliance Leader from 2003-2006. He was the recipient/co-recipient of the 2007 IEEE AP-S Symposium Best Student Paper Award, the 2007 IEEE IMS Third Best Student Paper Award, the 2007 ISAP Poster Presentation Award, the 2006 IEEE MTT Outstanding Young Engineer Award, the 2006 Asian-Pacific Microwave Conference Award, the 2004 IEEE Transactions on Advanced Packaging Commendable Paper Award, the 2003 NASA Godfrey "Art" Anzic Collaborative Distinguished Publication Award, the 2003 IBC International Educator of the Year Award, the 2003 IEEE CPMT Outstanding Young Engineer Award, the 2002 International Conference on Microwave and Millimeter-Wave Technology Best Paper Award, the 2002 Georgia Tech-ECE Outstanding Junior Faculty Award, the 2001 ACES Conference Best Paper Award, the 2000 NSF CAREER Award, and the 1997 Best Paper Award of the International Hybrid Microelectronics and Packaging Society. He was also the 1999 Technical Program Co-Chair of the 54th ARFTG Conference, Atlanta, GA, and the Chair of the 2005 IEEE CEM-TD Workshop. He is the Vice Chair of the RF Technical Committee (TC16) of the IEEE CPMT Society. He has organized various sessions and workshops on RF/wireless packaging and integration, RFIDs, and numerical techniques and wavelets in IEEE ECTC, IMS, VTC, and AP-S symposia, in all of which he was a member of the Technical Program Committee. He was the Technical Program Committee Chair for IEEE IMS 2008 Symposium. He is an Associate Editor of *IEEE Transactions on Advanced Packaging*. Dr. Tentzeris was a Visiting Professor with the Technical University of Munich, Germany, for the summer of 2002, where he introduced a course in the area of "High-Frequency Packaging." He has given more than 50 invited talks in the same area to various universities and companies in Europe, Asia, and America. He is a Senior Member of the IEEE, a member of USNC/URSI Commission D, a member of the MTT-15 committee, an Associate Member of EuMA, a Fellow of the Electromagnetics Academy, and a member of the Technical Chamber of Greece. 